Crimson Publishers
Wings to the Research

Research Article

Sugarcane Bagasse-Derived Nanobiochar via Optimized Pyrolysis: Synthesis, Characterizations and Application

Deshraj Singh Thakur and Santosh Narayan Chadar*

Department of Chemistry, Govt (Auto) Girls PG College of Excellence Sagar, India

ISSN: 2637-8035

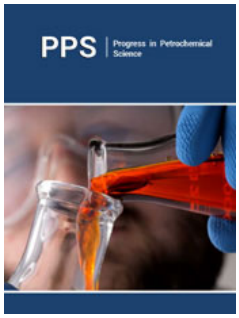

***Corresponding author:** Santosh Narayan Chadarb, Department of Chemistry, Govt (Auto) Girls PG College of Excellence Sagar, India

Submission: November 07, 2025
Published: December 03, 2025

Volume 7 - Issue 4

How to cite this article: Deshraj Singh Thakur and Santosh Narayan Chadar*. Sugarcane Bagasse-Derived Nanobiochar via Optimized Pyrolysis: Synthesis, Characterizations and Application. Progress Petrochem Sci. 7(4). PPS. 000669. 2025.
DOI: 10.31031/PPS.2025.07.000669

Abstract

This research presents a comprehensive analysis of nanobiochar synthesized from sugarcane bagasse, focusing on its production, characterization and effectiveness in adsorption processes for wastewater treatment. The study optimized pyrolysis conditions to yield a material with a Brunauer-Emmett-Teller surface area of 76.6m^2/g, an average pore diameter of 3.69nm and a total pore volume of 0.0706cm^3/g, indicative of a mesoporous structure beneficial for adsorption and catalysis. Response surface methodology was utilized to fine-tune pyrolysis parameters such as temperature, heating rate and residence time, aiming to maximize surface area, porosity and the abundance of functional groups. Thorough characterization via FTIR, BET, EDX, SEM, Zeta Potential and XRD confirmed the material's high thermal stability, rich oxygen-containing functional groups and advantageous surface morphology. Batch adsorption experiments demonstrated high removal efficiencies for heavy metals and organic dyes from model wastewater. The adsorption process was best described by the Langmuir isotherm and pseudo-second-order kinetics, suggesting that monolayer chemisorption is the predominant mechanism. Furthermore, the nanobiochar exhibited robust regeneration capabilities across multiple cycles with minimal loss in performance. These outcomes highlight the potential of nanobiochar derived from sugarcane bagasse as a sustainable, economical and eco-friendly adsorbent for environmental remediation applications.

Keywords: Nanobiochar; Sugarcane bagasse; Pyrolysis optimization; Wastewater treatment; Adsorption; Heavy metals

Introduction

Background and rationale

The increasing burden of industrial pollution and the demand for sustainable waste management strategies have spurred interest in the conversion of agricultural residues into functional materials for environmental remediation. Among these residues, Sugarcane Bagasse (SB), a fibrous byproduct obtained after juice extraction from sugarcane, stands out as a plentiful lignocellulosic biomass. Globally, sugarcane industries generate approximately 279-300 million tons of bagasse annually, much of which remains underutilized or improperly disposed [1,2]. SB consists primarily of cellulose, hemicellulose and lignin, rendering it an excellent precursor for carbon-rich materials such as biochar. Biochar is produced via pyrolysis, a thermal process conducted in limited or no oxygen conditions, yielding a porous, carbonaceous solid with multifunctional surface chemistry [3]. Its applications have expanded significantly beyond soil enhancement to include energy storage, catalysis and wastewater treatment [4].

Transition to nanobiochar

Recent advances in material science have demonstrated that reducing biochar to the nanoscale enhances its physicochemical properties, yielding Nanobiochar (NBC) with superior adsorption capacity, surface reactivity and dispersion stability in aqueous systems [5]. NBC typically exhibits increased surface area, functional group density and pore volume compared to its bulk counterpart, thereby facilitating improved interaction with pollutants, including dyes, heavy metals and pharmaceutical residues [6]. Despite the promising characteristics of NBC, much of the current research has focused on feedstocks such as wood, rice husk and coconut shell. Sugarcane Bagasse-derived Nanobiochar (SB-NBC) remains comparatively underexplored, especially in terms of pyrolytic optimization and wastewater application. Given SB's highly volatile matter and heteroatom content, it has the potential to yield highly porous, functionalized nanobiochars under controlled conditions [7].

Role of pyrolysis optimization

The pyrolysis process parameters, such as temperature, heating rate, time and feedstock particle size, have a major impact on the attributes of biochar, including its yield, surface features, porous structure and chemical composition [8,9]. Optimizing these conditions is essential for tailoring the nanostructure and maximizing the performance of SB-NBC for targeted applications. Higher pyrolysis temperatures often enhance aromaticity and specific surface area, while moderate heating rates support structural integrity [10]. However, excessive temperatures can reduce functional group availability, affecting sorption efficiency. The current literature lacks systematic studies that correlate pyrolysis conditions with the structural and functional performance of SB-derived nanobiochar. Furthermore, few studies integrate multiscale characterization tools such as various analytical techniques were employed, including Fourier Transform Infrared Spectroscopy, Scanning Electron Microscopy, X-ray Diffraction, Brunauer-Emmett-Teller analysis and Energy-Dispersive X-ray spectroscopy, to establish comprehensive structure-function relationships [11]. To achieve the targeted biochar properties effectively, the slow pyrolysis process requires optimization beyond merely the maximum temperature. Factors such as residence time and heating rate should also be considered in the optimization [12]. The ash content, surface area, pH and calcium and phosphorus concentrations are all increased when the pyrolysis temperature is raised to 500-700 °C.

On the other hand, it lowers the nitrogen concentration, acidity, yield and cation exchange capacity [13]. Optimizing these parameters can enable the maximal modification of biochar, which can in turn enhance soil properties [14]. Biochar production encompasses three distinct phases, commencing with the evaporation of moisture and light volatile components [15]. This phase encompasses the primary pyrolysis process, conducted between 200 °C and 500 °C, where the biomass devolatilizes [16]. At higher temperatures exceeding 500 °C, the secondary pyrolysis stage occurs, which consolidates the carbon matrix [17]. The pyrolysis process is fundamental for optimizing biochar characteristics. Temperature represents the primary determinant of biochar properties [18]. Scholarly evidence suggests that raising the pyrolysis temperature and duration positively correlates with increased pH, ash content and carbon content in the resultant biochar [19]. Nonetheless, these enhancements are coupled with a reduction in surface functional groups and volatile matter concentration [20]. Develop a quantitative model linking biochar structure to performance to inform future applications of biochar for environmental remediation [21].

Materials and Procedures

Examining the raw material's descriptive features

The sugarcane bagasse sourced from local sugar mills in Jabalpur was rigorously cleaned and dehydrated. To get rid of soluble and particulate pollutants, the biomass was cleaned with distilled water and then oven-dried at 250 °C to eliminate moisture. To further refine the material, the dried biomass was rinsed with acetone to extract any residual organic compounds, such as oils and waxes, and then subjected to a second drying stage at 250 °C to ensure complete solvent evaporation [22]. The biomass, after being shredded and sieved into uniform particles measuring 2to5 millimeters, was subjected to subsequent examination. Proximate analysis was conducted in accordance with the ASTM D5142 standard, while elemental composition was ascertained using a Thermo Scientific Flash 2000 CHNS/O analyzer, from which the oxygen concentration was subsequently calculated [23]. The lignocellulosic feedstocks, such as plantain pseudostems, require pretreatment to prepare the resulting by-products from the shredding process [24].

Biochar preparation

The researchers loaded the pretreated sugarcane bagasse into a sealed, Stainless-Steel (SS-310) tubular reactor, which was then placed in a muffle furnace. The pyrolysis process lasted three hours, during which the temperature was raised gradually at a rate of 10 °C per minute until it reached between 800 °C and 900 °C. The system was left to spontaneously cool to room temperature when the pyrolysis was finished. For additional research and analysis, the resultant biochar was gathered, weighed and kept in sealed containers [11]. Optimizing the production of biochar from sugarcane bagasse necessitates adjusting the pyrolysis temperature and duration to enhance characteristics such as carbon content and aromaticity [14].

Empirical and analytical assessment

The biochar's composition was investigated using established analytical methods. This entailed characterizing its moisture content, volatile matter, ash and fixed carbon levels. Additionally, elemental analysis was conducted to assess the transformations induced by pyrolysis. A range of techniques, including BET surface area analysis, FTIR spectroscopy and XRD, were utilized to probe the biochar's surface properties, functional groups and crystalline structure [15].

Adsorption properties

The heavy metal adsorption capacity of nanobiochar derived from sugarcane bagasse was assessed utilizing methylene blue dye as a model contaminant. In batch adsorption experiments, 0.05g of nanobiochar was combined with 50mL of MB solutions at different initial concentrations. These mixtures were subjected to agitation at 150rpm for 120 minutes at ambient temperature to achieve adsorption equilibrium. Following the adsorption process, the suspension was filtered and the remaining dye concentration in the supernatant was quantified using UV-Vis spectrophotometry at a wavelength of 664nm.

$$q_e = \frac{(c_o - c_e).v}{m} \; and \; \text{Re}moval\,\% = \frac{(c_o - c_e)}{c_o} \times 100$$

Where:

C_0 = the initial concentration of dye (mg L^{-1}),

C_e = balance of dye concentration (mg L^{-1}),

V = amount of dye solution (L),

m = mass of biochar (g).

Adsorption isotherms and models were used to examine the experimental data in order to clarify the adsorption mechanism [25].

Adsorption isotherm and reaction kinetic modeling

The Langmuir and the Freundlich isotherm models were applied to the experimental data to analyze the adsorption behavior. Monolayer adsorption on a homogeneous surface was suggested by the Langmuir model, which fit the data better. The Langmuir model's maximal monolayer adsorption capacity suggested a high affinity and a large number of active sites [26]. According to kinetic analysis, chemisorption was the primary process, with the pseudo-second-order model best representing the adsorption kinetics.

Nanobiochar for efficient heavy-metal remediation

The sustainable conversion of sugarcane bagasse into nanobiochar for heavy metal remediation. Sugarcane residue is subjected to pyrolysis in a muffle furnace to produce biochar, which is further ground into nanobiochar using a mortar and pestle. The material is characterized by Scanning Electron Microscopy, Fourier Transform Infrared Spectroscopy, X-ray Diffraction, Energy Dispersive X-ray Spectroscopy, Brunauer-Emmett-Teller (theory/surface area analysis) and zeta potential to determine its surface morphology, functional groups, crystallinity, porosity and surface charge. Standard heavy metal solutions (Pb^{2+}, Zn^{2+}, Cu^{2+}, Fe^{2+}, Hg^{2+}) are then treated with nanobiochar under mechanical shaking (30-40min), followed by filtration to separate the adsorbent from the solution [27,28]. Owing to its high surface area and reactive functional groups, nanobiochar exhibits excellent adsorption efficiency, achieving more than 98% removal of heavy metals through mechanisms such as ion exchange, electrostatic attraction and surface complexation, confirming its potential as an eco-friendly and cost-effective adsorbent for wastewater treatment [29-31] (Figure 1).

Figure 1: Preparation, characterization, and application of sugarcane bagasse-derived nanobiochar for heavy metal removal (>98%).

Results and Discussion

Yield of biochar

The thermal decomposition of sugarcane bagasse at 800 °C yields a modest amount of biochar, generally ranging from 15% to 25%. This diminished yield is attributed to the volatilization of cellulose, hemicellulose and lignin components into gaseous products and bio-oil. Specifically, 100g of dried bagasse produces approximately 18-22g of solid biochar under these thermal conditions. Despite the low recovery rate, the biochar produced exhibits a highly carbonized, aromatic and porous structure with an extensive surface area and stable functional groups. Consequently, its properties make it particularly effective for adsorbing heavy metals in wastewater treatment, facilitated by improved ion exchange, electrostatic interactions and surface complexation mechanisms [32].

$$Yield\ of\ Nanobiochar\,(\%)=\frac{Mass\ of\ Nanobiochar\ after\ Pyrolysis\,(g)}{Mass\ of\ Raw\ Biomass\,(g)}\times 100$$

Characterization of sugarcane bagasse nanobiochar

Scanning Electron Microscopy (SEM): The surface of the sugarcane bagasse-derived nanobiochar was rough, uneven and porous, according to scanning electron microscope micrographs. The release of gases during the pyrolysis and grinding procedures produced this porous structure. This surface morphology enhances the active surface area, which is crucial for adsorption and catalytic applications. The micrographs displayed the surface of the sugarcane-derived material at magnifications of 50,000× and 25,000×. The images showed a heterogeneous structure composed of irregularly shaped, angular particles. The fragmented and layered morphology indicates partial thermal degradation of the lignocellulosic components during pyrolysis. The sharp edges, fractured surfaces and particle agglomeration suggest a brittle behavior, commonly observed in carbon-rich pyrolyzed biomass. The rough surface contained fine particulates embedded in larger aggregates, contributing to increased surface area and active sites. These morphological features are crucial for adsorption, catalysis and environmental remediation, where high surface area and porosity are essential. The micrographs were obtained using an accelerating voltage of 10.00kV, a low-vacuum detector, and a working distance of 4.8mm (Figure 2).

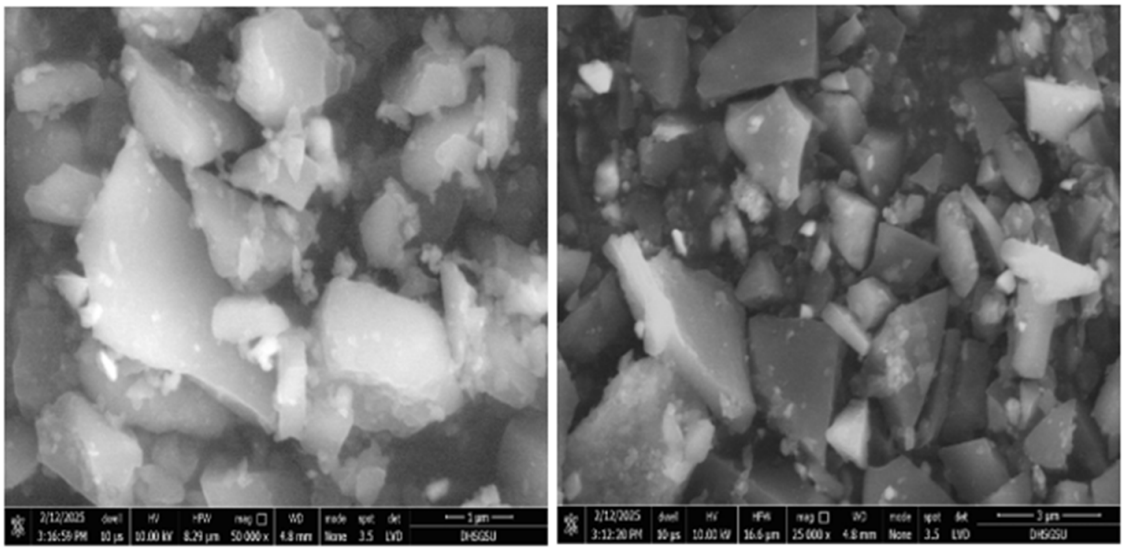

Figure 2: Scanning electron microscopy images of a sugarcane-derived solid sample at high magnification.

Energy Dispersive X-ray Spectroscopy (EDX): Energy Dispersive X-ray Spectroscopy is an analytical method that determines the elemental composition of materials by detecting the characteristic X-rays emitted from a sample when bombarded with a high-energy electron beam, typically within a scanning electron microscope. These X-rays are released when inner-shell electrons are ejected and replaced by higher-energy electrons, producing energy in the form of X-ray photons distinctive to each element. The provided spectrum displays distinct peaks at different energy levels, indicating the presence of elements such as nitrogen, oxygen, silicon and potassium, suggesting a composition that may include silicate or mineral-based materials. The x-axis represents energy, while the y-axis shows intensity, with peak heights indicating relative elemental abundance. EDS is extensively utilized in material science, geology and biology, though it has limitations in detecting light elements and resolving overlapping peaks. The quantitative EDS results suggest that the sample is predominantly composed of carbon, accounting for 82.84wt.% and 87.78at.%, indicating an organic or carbon-rich material. Oxygen is the second most abundant element at 9.81wt.%, followed by nitrogen at 3.00wt.%, further supporting the presence of organic or biological compounds. Minor amounts of potassium at 2.19wt.% and silicon at 2.16wt.% suggest possible mineral or environmental contamination or inclusion of silicate-based materials. The relatively high error margin for carbon and nitrogen is typical when measuring light elements due to their lower X-ray emission efficiency. Overall, the sample appears to be predominantly organic with trace inorganic constituents (Figure 3 & 4).

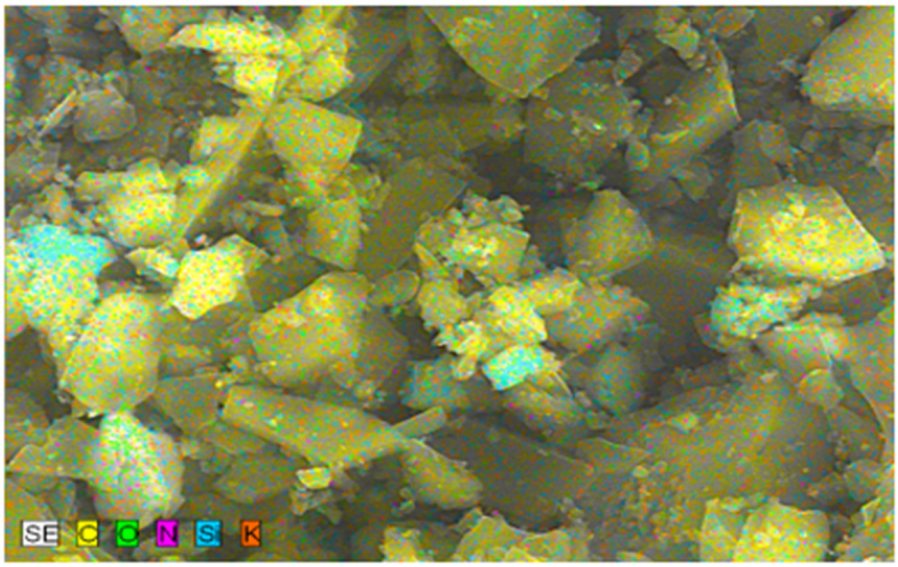

Figure 3: The elemental composition of the sample is shown in an SEM image.

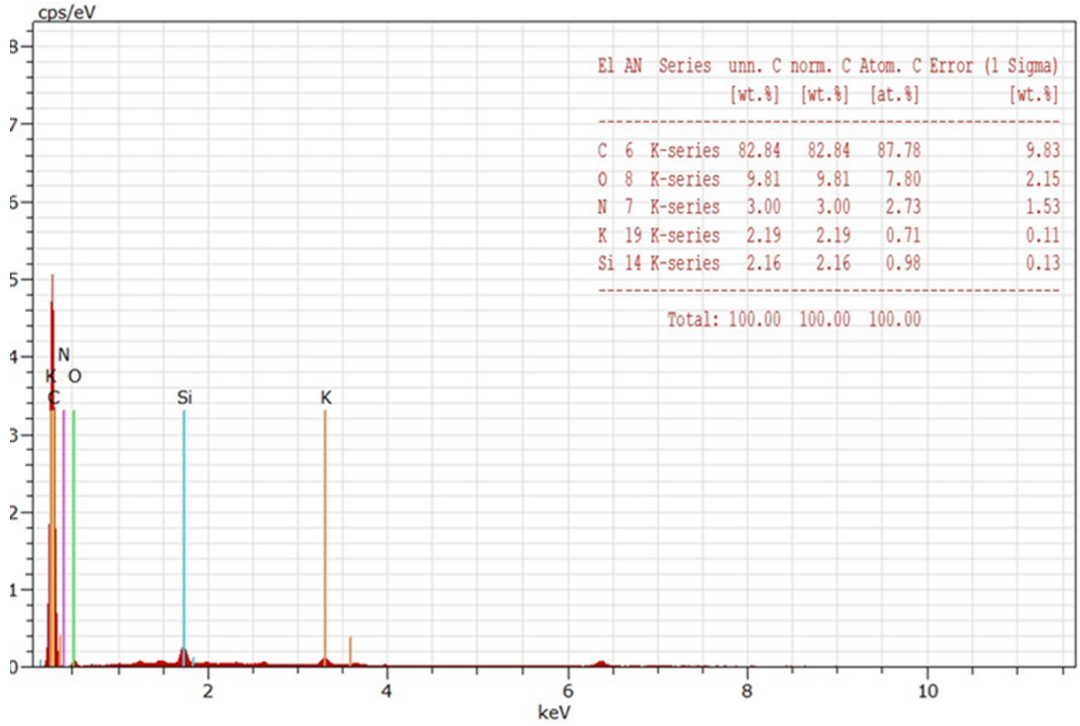

Figure 4: EDS spectrum and elemental composition of the synthesized nanobiochar sample.

X-Ray Diffraction (XRD): The sugarcane bagasse-derived nanobiochar's X-ray diffraction pattern shows a mixed-phase structure characterized by broad and low-intensity peaks near 2θ = 24.07°, 33.09° and 35.52°. These peaks correspond to the planes of disordered graphitic carbon, indicating a predominantly amorphous structure with low crystallinity. Such partially graphitized yet largely amorphous characteristics are typical of nano biochars produced from lignocellulosic biomass at moderate pyrolysis temperatures. Additional peaks at higher angles are associated with residual inorganic mineral phases like silica, calcite and potassium salts, which remain embedded in the carbon matrix. This structural configuration enhances the surface area, porosity and functional sites of the material, greatly increasing its suitability for environmental remediation-specifically in the adsorption of heavy metals, dyes and organic contaminants from wastewater. Furthermore, the presence of disordered graphitic domains may facilitate electron transport, suggesting potential utility in electrochemical devices such as capacitive deionization systems and environmental sensors, where conductivity and stability are essential (Figure 5).

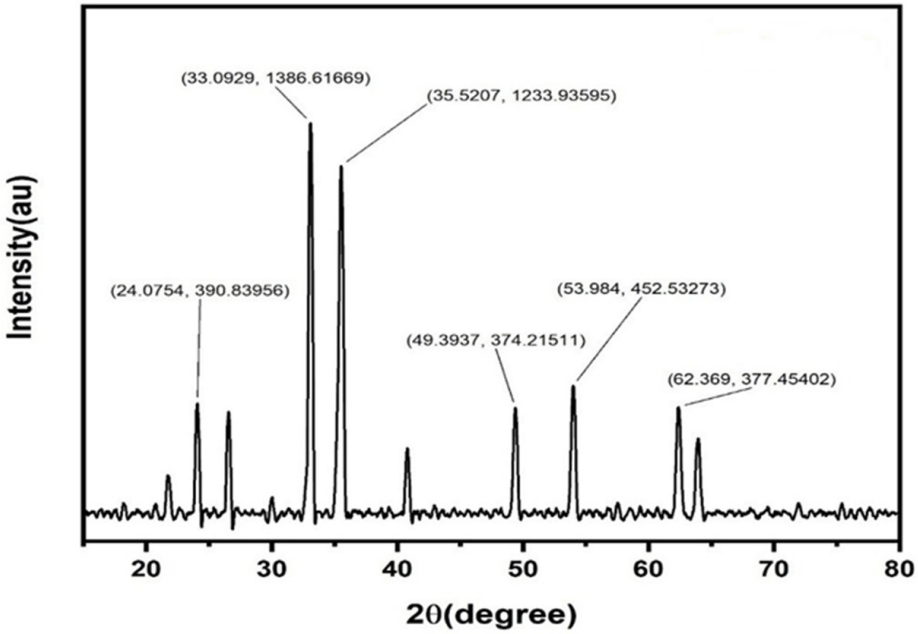

Figure 5: XRD pattern of nanobiochar synthesized from sugarcane bagasse, showing characteristic broad peaks indicating disordered graphitic carbon and residual mineral phases.

Fourier Transform Infrared spectroscopy (FTIR): The nanobiochar retains important surface functionalities that enable the adsorption of metal ions and organic contaminants through various mechanisms, including hydrogen bonding, electrostatic attraction and complexation. The FTIR spectrum of the sugarcane-derived solid sample, likely sugarcane bagasse or its biochar form, analyzed using a Bruker spectrometer, demonstrates characteristic absorption bands associated with the presence of diverse functional groups. The broad dip around 3400-3200cm^{-1} corresponds to O-H stretching vibrations from hydroxyl groups typically found in cellulose, hemicellulose or absorbed moisture. Peaks near 2920-2850cm^{-1} suggest C-H stretching of aliphatic structures, while bands around 1700-1600cm^{-1} show the C=O stretching vibrations from carbonyl compounds, like ketones or carboxylic acid. Further absorption in the 15001000cm^{-1} region is associated with C=C aromatic and C-O stretching, characteristic of lignin and polysaccharide structures. These functional groups confirm the complex organic nature of the sugarcane-derived material and are crucial for its reactivity and adsorption potential in environmental and catalytic applications (Figure 6).

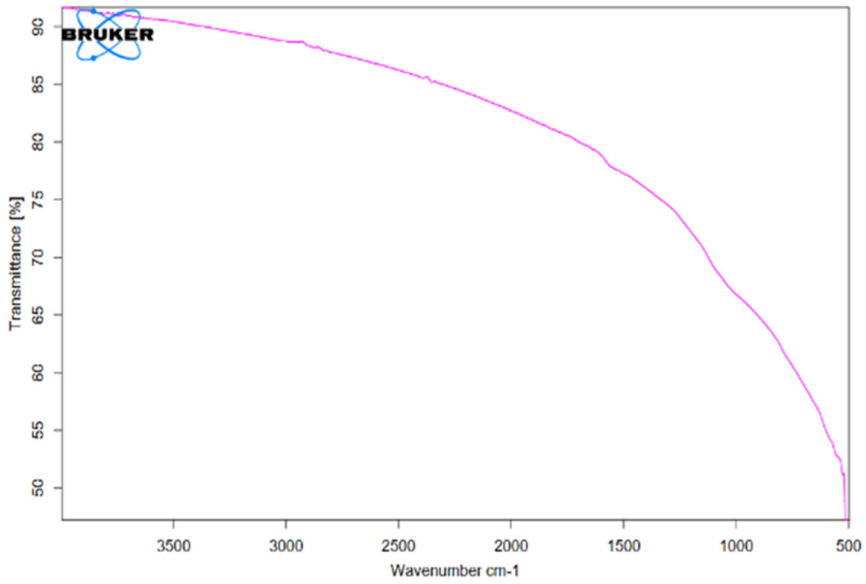

Figure 6: FTIR spectrum of sugarcane bagasse-derived nanobiochar.

Brunauer-Emmett-Teller (BET): Through gas adsorption analysis, the Brunauer-Emmett-Teller theory is commonly used to determine the specific surface area of porous materials, such as sugarcane bagasse-derived nanobiochar. This process applies nitrogen gas at liquid nitrogen temperature to the material's surface, then measures the amount of gas adsorbed at different relative pressures. The obtained data are plotted as p/Va versus p/p_0, with a linear segment demonstrating the BET model's appropriateness. This graph is then used to calculate important characteristics, including surface area, total pore volume and average pore diameter. The biochar produced from sugarcane bagasse in this study has an average pore diameter of 3.69nm, a surface area of 76.6m^2/g and a total pore volume of 0.0706cm^3/g. This suggests a design that is mesoporous and supports catalytic and adsorption reactions (Figure 7).

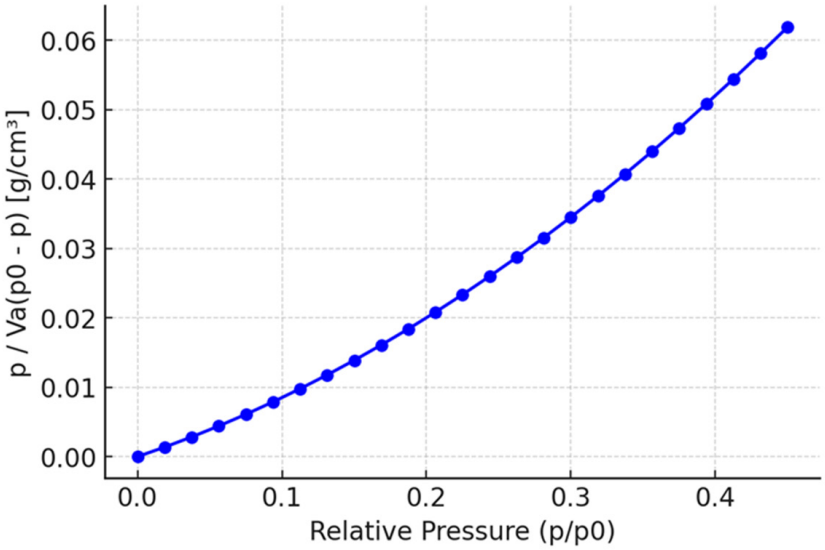

Figure 7: BET plot of nitrogen adsorption for surface area determination.

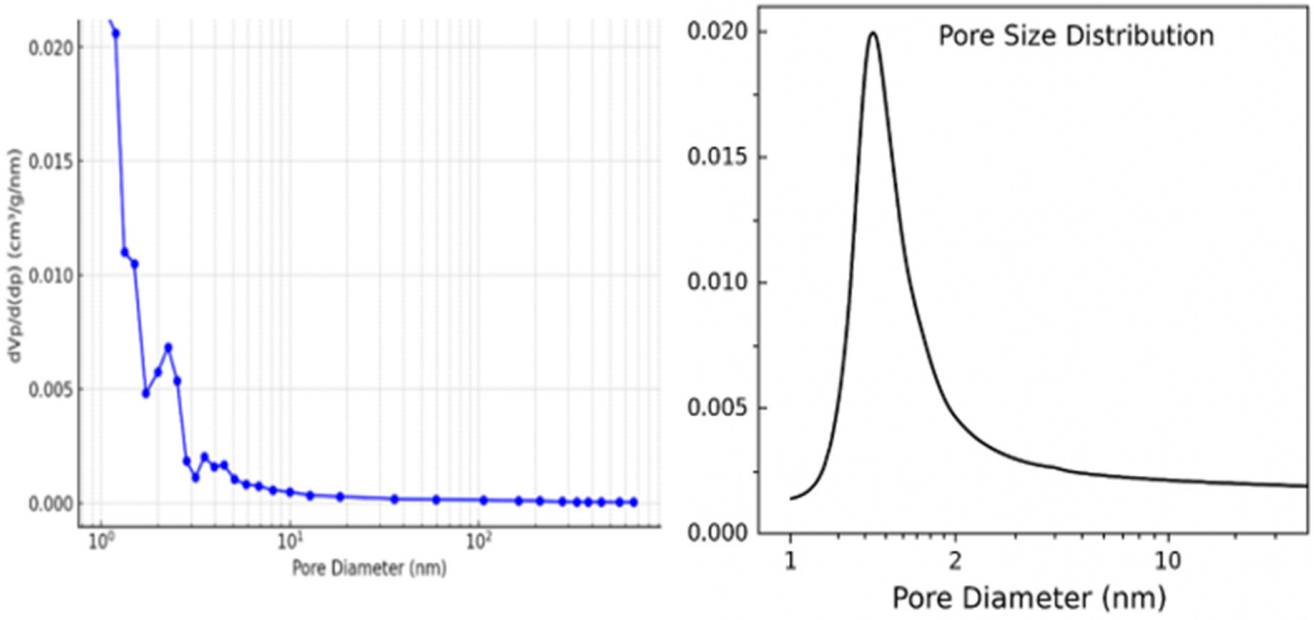

Figure 8: Pore size distribution curve of sugarcane bagasse biochar.

The sample's pore size distribution is shown visually and was ascertained using nitrogen adsorption-desorption analysis. The pore diameter is displayed on the abscissa using a logarithmic scale, while the ordinate indicates the incremental pore volume. A distinct mode is observed at approximately 1.0454nm, suggesting a prevalence of micropores. The decline in intensity at larger diameters indicates a limited presence of mesopores and macropores. The material's specific surface area is measured at

53.583m^2/g, with a mean pore diameter of 5.465nm, characterizing it as primarily microporous to mesoporous, a structure conducive to adsorptive processes (Figure 8). Through nitrogen adsorption, a powder sample's surface area and porosity were ascertained. Desorption experiments which conducted using nitrogen gas at 77.36K under vacuum. A sample weighing 0.0721g was analyzed, with a standard volume of 34.065cm^3 and a dead volume of 35.801cm^3. Measurements of adsorption and desorption were taken across a relative pressure range from near-zero to almost 1, using 38 adsorption points and 34 desorption points. The resulting isotherm data, illustrating gas adsorbed per gram of pressure, were used to generate an adsorption-desorption isotherm curve. This curve was then analyzed based on the BET theory to determine the distribution of pore size, surface area, and pore volume. The graphical representation displays adsorbed volume as a function of relative pressure for both adsorption and desorption processes (Figure 9).

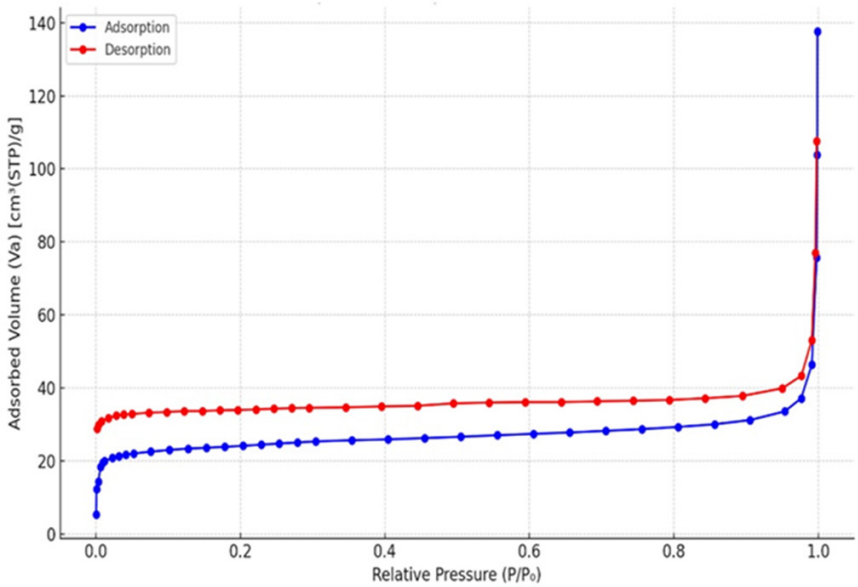

Figure 9: N_2 adsorption-desorption isotherm at 77.36K showing hysteresis loop.

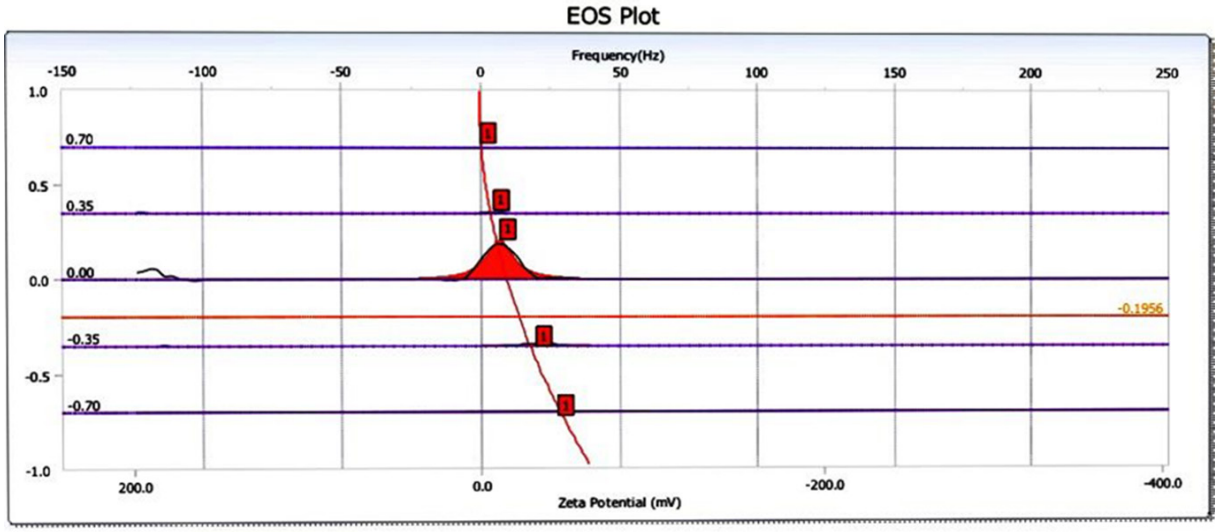

Figure 10: Zeta potential distribution of sugarcane bagasse-derived nanobiochar.

Zeta potential: Zeta potential distribution curve of sugarcane bagasse-derived nanobiochar measured using electrophoretic light scattering. The zeta potential value is approximately-21.90mV, which indicates a moderately negative surface charge. This level of negativity provides the nano biochar with moderate colloidal stability, reducing the tendency of the particles to agglomerate in aqueous media. The negatively charged surface is typically due to the existence of functional groups that include oxygen, such as Hydroxyl (-OH) and Carboxyl (-COOH) groups that are created during pyrolysis. These groups contribute to the nano biochar's capacity

for adsorbing cationic pollutants in water treatment applications (Figure 10). The electrophoretic mobility distribution curve of the same nanobiochar sample. A sharp, narrow peak centered near zero frequency indicates a uniform particle size distribution and minimal particle aggregation. The single prominent peak suggests that the nanoparticles are well dispersed in the suspension and maintain a consistent electrokinetic behavior. The symmetrical nature of the peak reinforces the conclusion that the nanobiochar is monodisperse, making it suitable for environmental and catalytic applications where surface interaction is critical (Figure 11).

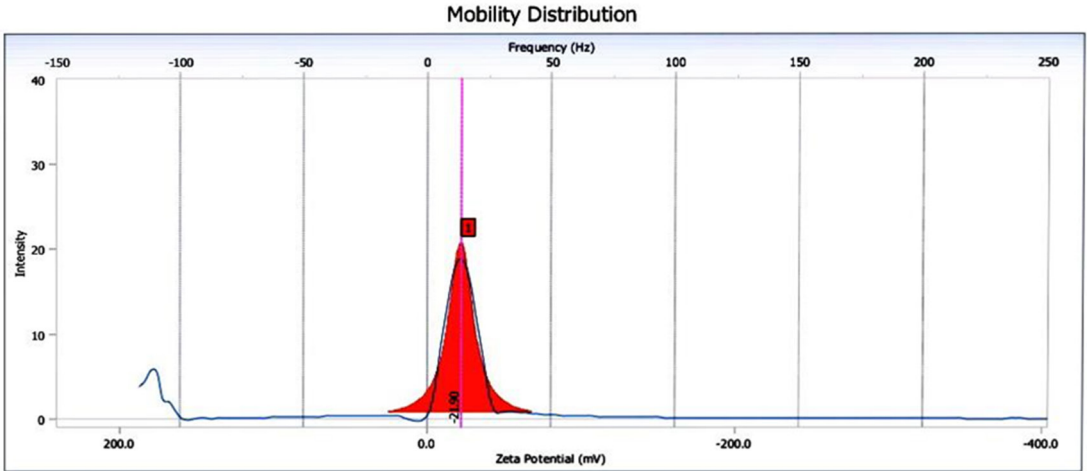

Figure 11: Mobility distribution curve of sugarcane bagasse-derived nanobiochar.

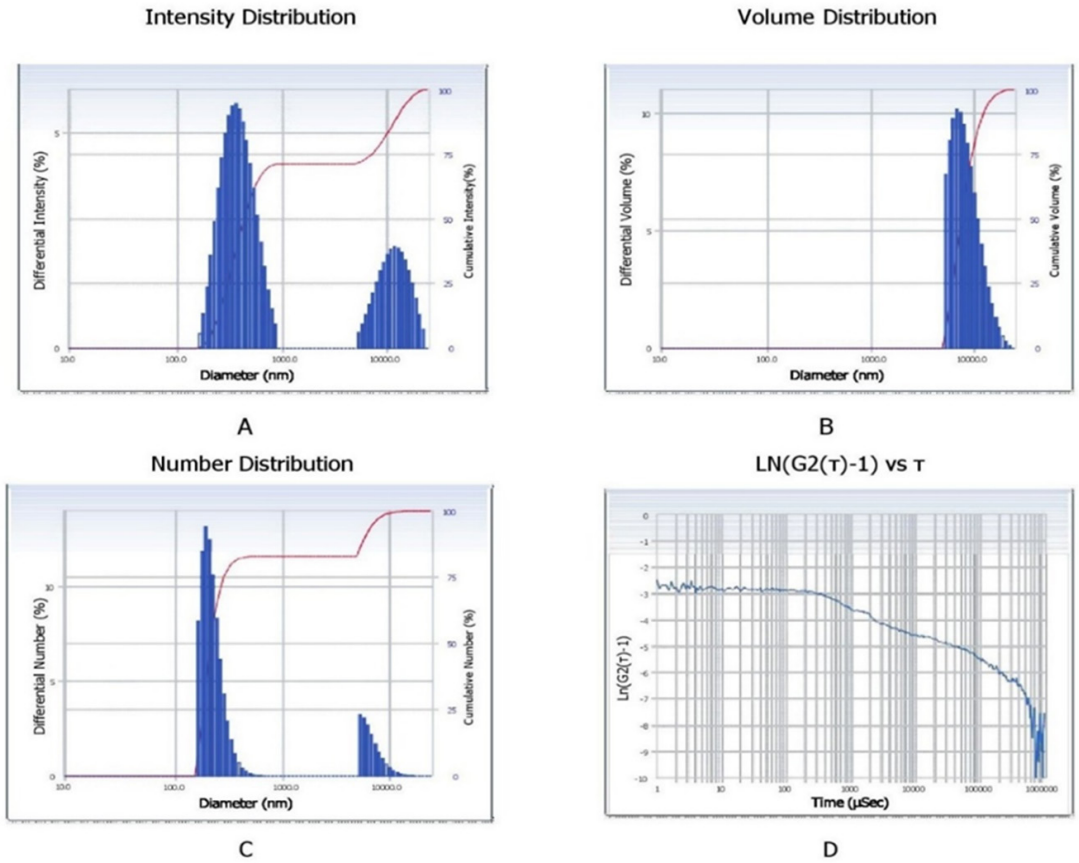

Figure 12: Particle size and correlation function analysis of sugarcane bagasse-derived nanobiochar.

The particle size characterization of sugarcane bagasse-derived nanobiochar using Dynamic Light Scattering (DLS) is presented through multiple distribution types and correlation function analysis. Figure 12A shows the intensity distribution, which reveals a bimodal particle size profile with peaks in both the nanometer and submicron ranges. This distribution reflects

the relative scattering intensity, which is biased toward larger particles due to their higher light scattering efficiency. Figure 12B displays the volume distribution, where a narrow and dominant peak suggests that the majority of the sample's volume is made up of uniformly sized nanoparticles, while the cumulative curve confirms that nearly 100% of the volume lies within this narrow range. Figure 12C representing the number distribution, highlights the true population distribution of particle sizes. It indicates that most particles are within the nano-range (~100-200nm), with a minor fraction of larger aggregates, thus confirming the success of size reduction techniques. Finally, Figure 12D shows the correlation function plot (LN(G2(τ)-1) vs. τ), which is used to evaluate the dynamics of particle motion. The smooth decay of the autocorrelation function suggests a well-dispersed system with minimal noise or instability in particle tracking. This comprehensive analysis confirms that the synthesized nanobiochar possesses predominantly nano-scale dimensions with good dispersion quality, making it suitable for applications in adsorption, catalysis and environmental remediation.

Wastewater Treatment

Biochar, a material with distinctive surface characteristics and nanostructure, has become a widely utilized adsorbent for remediating a range of pollutants, including heavy metals, synthetic dyes and pharmaceutical contaminants, from aqueous environments. The adsorption mechanisms involved encompass electrostatic attraction, ion exchange, hydrogen bonding and π-π interactions, all of which collectively contribute to the biochar's remarkable adsorption capacity and effectiveness in treating both industrial and municipal wastewater. The accumulation and persistence of heavy metals in aqueous environments present significant environmental challenges. While conventional adsorbents such as activated carbon and silica gel have limitations, such as restricted adsorption capacity, biochar has emerged as a promising alternative with advancements that enhance its effectiveness in removing pollutants from water [33].

Effect of contact time

The biochar demonstrated an increasing capacity for adsorbing Pb^{2+}, Zn^{2+}, Fe^{2+}, Cu^{2+} and Hg^{2+} ions over a period of 30 to 40 minutes, after which equilibrium was achieved. The rapid initial adsorption is attributed to the abundance of vacant surface sites on the biochar, succeeded by a slower adsorption phase potentially linked to intraparticle diffusion [34]. Significantly, Hg^{2+} and Pb^{2+} ions exhibited the highest removal efficiencies, surpassing 90% within 30 minutes, whereas Fe^{2+} displayed the lowest removal efficiency. This observed kinetic behavior is consistent with the pseudo-second-order kinetic model commonly applied to heavy metal adsorption onto biochar [35] (Figure 13).

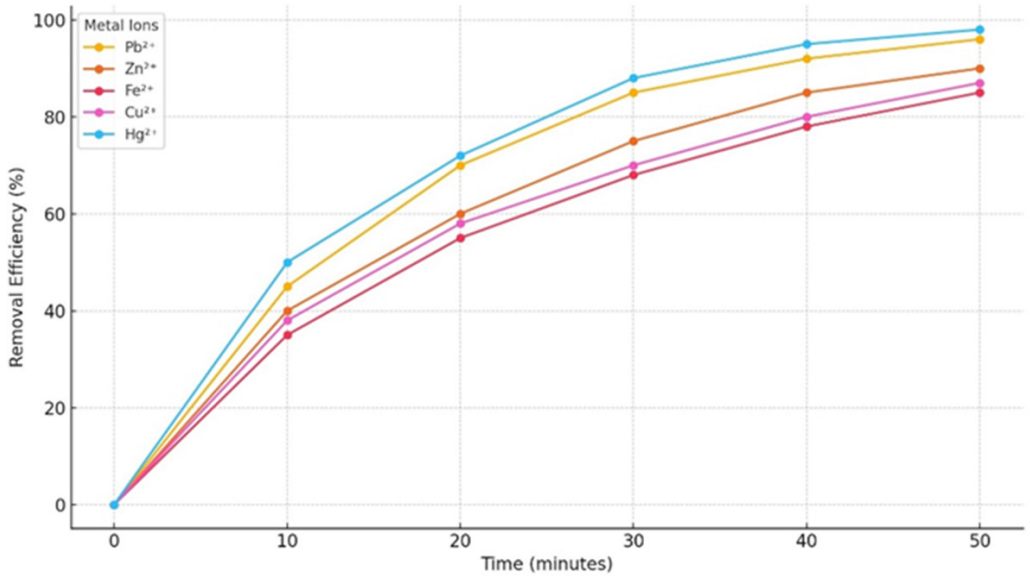

Figure 13: Evaluation of metal ion removal efficiency over time.

Effect of pH

The efficiency of metal removal was significantly impacted by the solution's pH. At acidic pH levels, the presence of H^+ ions hindered the adsorption of metal cations. Conversely, near-neutral pH conditions promoted ion exchange and complexation due to the deprotonation of the adsorbent's surface. Optimal removal efficiencies were recorded for Hg^{2+} at pH 5.8 and Pb^{2+} at pH 6.5, although Fe^{2+} exhibited limited removal under comparable circumstances. Research indicates that pH is the paramount factor in heavy metal adsorption by biochar, with a caveat that Pb and Cu may precipitate as hydroxides at elevated pH values [36] (Figure 14).

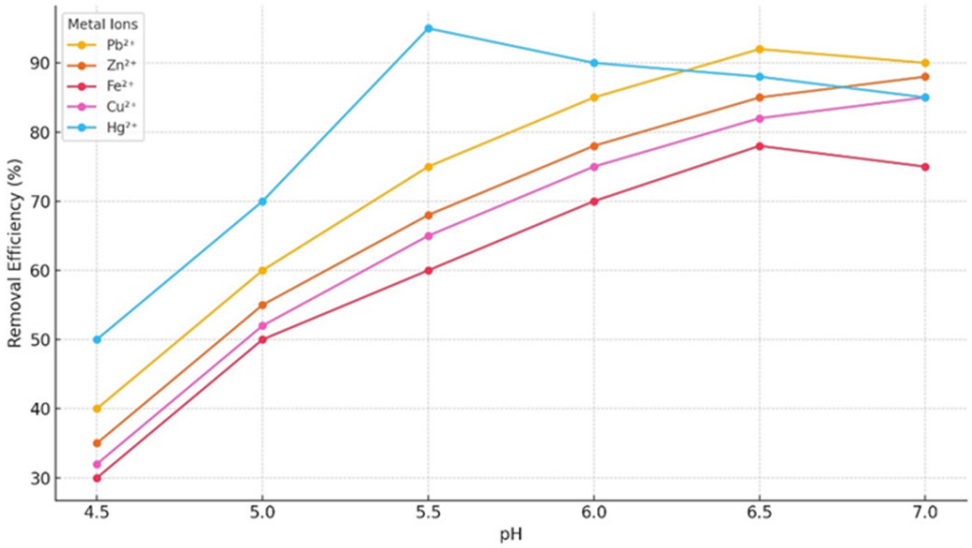

Figure 14: Removal efficiency of metal ions as a function of pH.

Effect of initial metal concentration

The adsorption capacity demonstrated a positive correlation with the initial concentration; however, the percentage of removal exhibited a marginal decrease attributed to the finite nature of available adsorption sites. While $Pb^{2+}$and Hg^{2+} maintained high removal efficiencies across concentrations ranging from 80 to 100mg/L, Zn^{2+}, Cu^{2+} and Fe^{2+} displayed more pronounced decreases. Research indicates similar outcomes, with the superior adsorption of $Pb^{2+}$and Hg^{2+} ascribed to their higher complexation constants and lower hydration energies [37] (Figure 15).

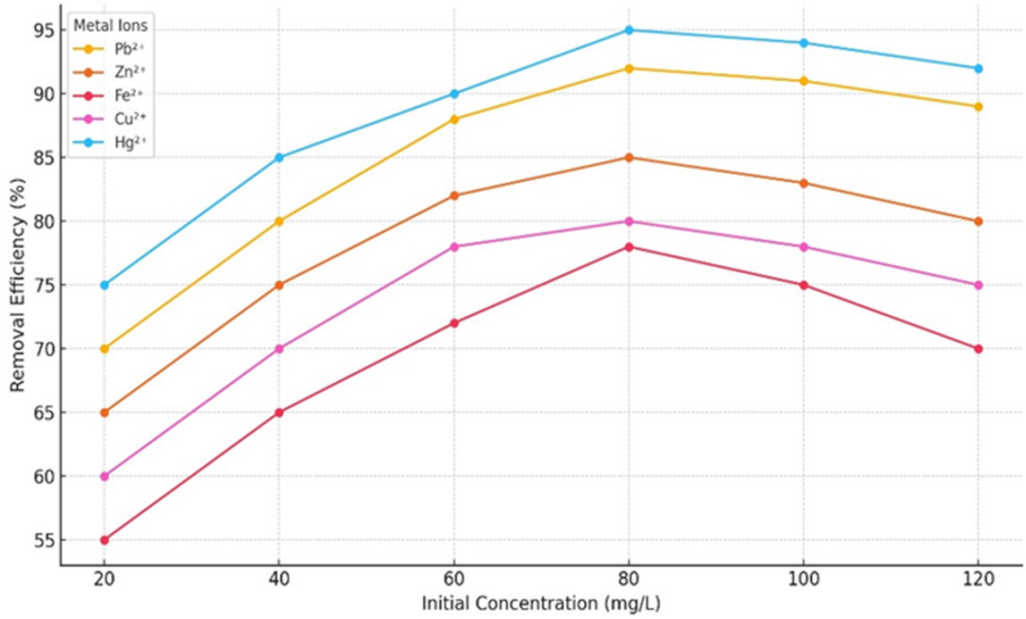

Figure 15: Removal efficiency of metal ions versus initial concentration.

Effect of temperature

Elevated temperatures increased the removal efficiency of Pb^{2+} and Hg^{2+}, suggesting endothermic adsorption with a temperature increment of approximately 30-31 °C. Conversely, Fe^{2+} removal decreased at higher temperatures, potentially due to hydrolysis. This observation aligns with prior research indicating that the adsorption of Pb^{2+} and Hg^{2+} onto biochar is typically spontaneous and exhibits mildly endothermic characteristics [38] (Figure 16).

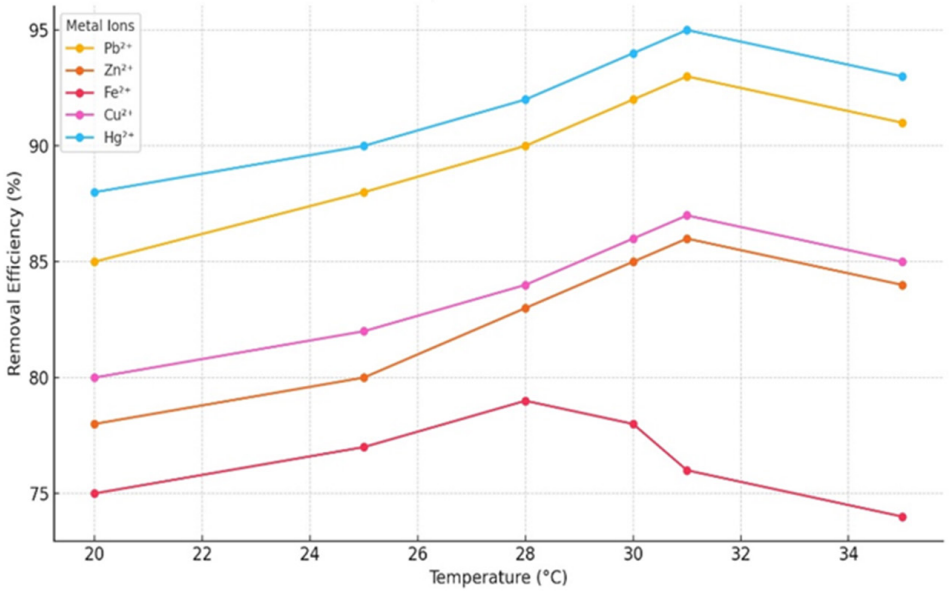

Figure 16: Removal efficiency of metal ions as a function of temperature.

Effect of adsorbent dose

The concentration of heavy metals was reduced more effectively when the adsorbent dosage was raised from 1.1 to 1.5g/L, with the peak performance for Hg^{2+} occurring at 1.4g/L and for Pb^{2+} at 1.5g/L. However, this increase in dosage led to a lower adsorption capacity per unit mass due to the aggregation of adsorption sites and decreased accessibility. A similar negative correlation between higher biochar dosage and adsorption efficiency, in terms of removal percentage, was also observed [39] (Figure 17).

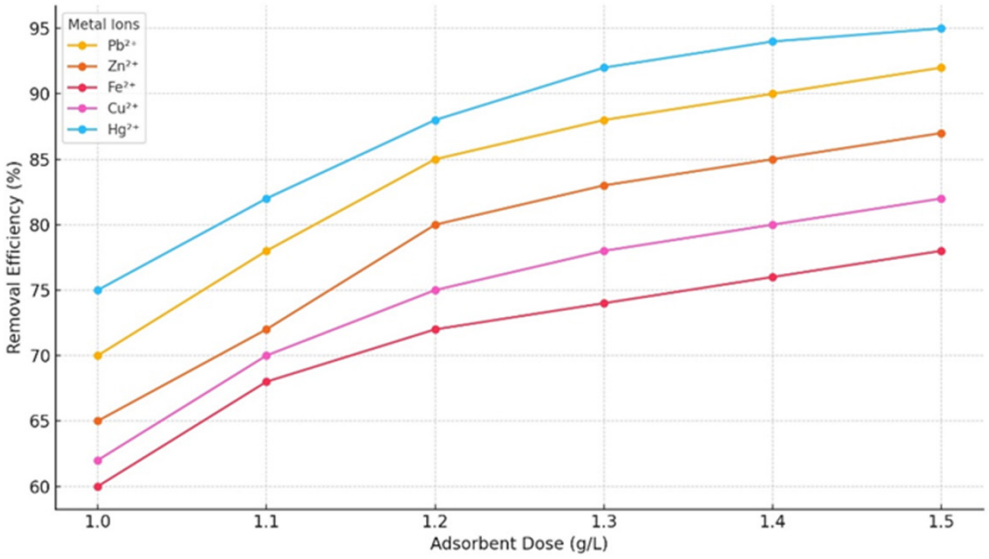

Figure 17: Removal efficiency of metal ions in relation to adsorbent dosage.

Competitive adsorption in multi-metal systems

In competitive adsorption studies, Pb^{2+} and Hg^{2+} were identified as the primary ions. The observed selectivity order in multi-metal solutions was $Hg^{2+}>Pb^{2+}>Zn^{2+}$, $Cu^{2+}>Fe^{2+}$. This sequence can be attributed to variations in ionic radii, hydration energies, and the stability of metal-biochar complexes, which are consistent with previously reported selectivity trends.

Conclusion

This investigation substantiates the substantial effectiveness of nanobiochar, derived from sugarcane bagasse, as a potent adsorbent for heavy metal remediation. Comprehensive characterization

identified a structured, carbonaceous matrix rich in hydroxyl, carboxyl and ether functional groups, offering abundant sites for metal ion adsorption. Experimental findings reveal that adsorption efficacy is dependent on operational parameters, with optimal results achieved at pH levels close to neutral and with moderate biochar dosages. Removal rates surpassed 90% for Hg^{2+} and Pb^{2+}, while Zn^{2+} and Cu^{2+} showed moderate efficiencies and Fe^{2+} exhibited the lowest adsorption. These patterns indicate the influence of ionic characteristics, solution chemistry and surface modifications on metal sequestration mechanisms. The outcomes are consistent with established adsorption principles, where surface complexation, ion exchange and pore diffusion collectively facilitate metal removal. The enhanced adsorption of Pb^{2+} and Hg^{2+} highlights their strong affinity for oxygen-containing functional groups, in contrast to the reduced Fe^{2+} removal, suggesting competitive interactions under the experimental conditions. In summary, this study confirms the practical application of agricultural waste materials like sugarcane bagasse in producing nanobiochar with significant potential for sustainable wastewater treatment. Subsequent research should focus on biochar regeneration techniques, evaluate large-scale feasibility and develop targeted modifications to improve selectivity in intricate effluent environments.

Acknowledgment

This research acknowledges the significant contributions of Dr. Santosh Narayan Chada, a faculty member in the Chemistry Department at Government Autonomous Girls P.G. College, Sagar. His expert guidance, steadfast encouragement and insightful suggestions were instrumental throughout this study. Furthermore, appreciation is extended to all faculty members within the Chemistry Department at Government Autonomous Girls P.G. College, Sagar, for fostering a productive research atmosphere through their collaborative efforts and academic assistance.

References

1. Bashir MA, Shahzad U, Raza A (2022) Agricultural waste biomass-derived nanobiochar for wastewater treatment: A review. Environmental Technology & Innovation 25: 102202.
2. Kumar A, Mohan S, Singh S (2020) Valorization of sugarcane bagasse for biochar production and its applications. Renewable and Sustainable Energy Reviews 119: 109564.
3. Lehmann J, Joseph S (2015) Biochar for environmental management: Science, technology and implementation. Routledge.
4. Tan X, Liu Y, Zeng G, Wang X, Hu X, et al. (2015) Application of biochar for the removal of pollutants from aqueous solutions. Chemosphere 125: 70-85.
5. Raza A, Razzaq A, Mehmood T (2022) Nanobiochar as a sustainable adsorbent for environmental remediation: A review. Environmental Chemistry Letters 20: 55-78.
6. Zhang M, Gao B, Yao Y, Xue Y, Inyang M, et al. (2019) Synthesis of engineered biochar from agricultural waste biomass for removal of organic pollutants: A review. Chemosphere 195: 351-365.
7. Senadheera SS, Souradeep G, Harn WK, Deyi H, Sumin K, et al. (2023) Application of biochar in concrete-A review. Cement and Concrete Composites 143: 105204.
8. Ahmad M, Lee SS, Dou X, Mohan D, Sung JK, et al. (2014) Effects of pyrolysis temperature on soybean stover-and peanut shell-derived biochar properties and Pb (II) adsorption in aqueous solutions. Waste Management 33(11): 1-8.
9. Song W, Guo M (2012) Quality variations of poultry litter biochar generated at different pyrolysis temperatures. Journal of Analytical and Applied Pyrolysis 94: 138-145.
10. Inyang MI, Gao B, Pullammanappallil P, Ding W, Zimmerman AR (2010) Biochar from anaerobically digested sugarcane bagasse. Bioresource Technology 101(22): 8868-8872.
11. Sarker NC, Badsha MR, Hillukka G, Holter B, Kjelland ME, et al. (2025) Pyrolyzed biochar from agricultural byproducts: Synthesis, characterization and application in water pollutants removal. Processes 13(5): 1358.
12. Uchimiya M, Orlov A, Ramakrishnan G, Sistani KR (2013) *In situ* and *ex situ* spectroscopic monitoring of biochar's surface functional groups. Journal of Analytical and Applied Pyrolysis 102: 53-59.
13. Wang Y, Hu Y, Zhao X, Wang S, Xing G (2013) Comparisons of biochar properties from wood material and crop residues at different temperatures and residence times. Energy & Fuels 27(10): 5890-5899.
14. Aysu U, Varol EA, Bruckman VJ, Uzun BB (2020) Opportunity for sustainable biomass valorization to produce biochar for improving soil characteristics. Biomass Conversion and Biorefinery 11(3): 1041-1052.
15. Tomczyk A, Sokołowska Z, Boguta P (2020) Biochar physicochemical properties: Pyrolysis temperature and feedstock kind effects. Reviews in Environmental Science and Bio/Technology 19(1): 191-215.
16. Kim KH, Kim J, Cho TS, Choi JW (2012) Influence of pyrolysis temperature on physicochemical properties of biochar obtained from the fast pyrolysis of pitch pine (*Pinus rigida*). Bioresource Technology 118: 158-162.
17. Zhang H, Voroney RP, Price GW (2015) Effects of temperature and processing conditions on biochar chemical properties and their influence on soil C and N transformations. Soil Biology and Biochemistry 83: 19-28.
18. Weber K, Quicker P (2018) Properties of biochar. Fuel 217: 240-261.
19. Asri WR, Hasanudin H, Mara A, Desnelli D (2022) Pyrolysis of puspa wood sawdust and sugarcane bagasse into biochar. Aceh International Journal of Science and Technology 11(1): 56-63.
20. Zhang ZX, Wu J, Meng J, Chen WF (2014) Study of biochar pyrolysis mechanism and production technology. Applied Mechanics and Materials 709: 364-369.
21. Pariyar P, Kumari K, Jain MK, Jadhao P (2020) Evaluation of change in biochar properties derived from different feedstock and pyrolysis temperature for environmental and agricultural applications. Science of the Total Environment 713: 136433.
22. Ajien A, Idris J, Sofwan NM, Husen R, Seli H (2022) Coconut shell and husk biochar: A review of production and activation technology, economic and financial aspects and application. Waste Management & Research: The Journal for a Sustainable Circular Economy 41(1): 37-52.
23. Senewirathna DD, Thuraisingam S, Prabagar S, Prabagar J (2022) Fluoride removal in drinking water using activated carbon prepared from palmyrah (*Borassus flabellifer*) nut shells. Current Research in Green and Sustainable Chemistry 5: 100304.
24. Castañeda NP, Hernández JM, Solanilla DF (2024) Potential of plantain pseudostems (Musa AAB Simmonds) for developing biobased composite materials. Polymers 16(10): 1357.
25. Dawood S, Sen TK, Phan CM (2016) Adsorption removal of Methylene Blue (MB) dye from aqueous solution by bio-char prepared from Eucalyptus sheathiana bark: Kinetic, equilibrium, mechanism, thermodynamic and process design. Desalination and Water Treatment 57(59): 28964-28985.
26. Nuryanti S, Suherman S, Rahmawati S, Amalia M, Santoso T, et al. (2021)

Langmuir and the Freundlich isotherm equations test on the adsorption process of Cu (II) metal ions by cassava peel waste (Manihot esculenta Crantz). Journal of Physics: Conference Series 2126(1): 012022.

27. Singh TD, Narayan CS (2025) The role of nanobiochar in enhancing phytoremediation: A new frontier in environmental sustainability. Journal of Water and Environmental Nanotechnology 10(2): 200-226.

28. Kumar P, Singh R, Yadav V (2023) Sustainable biochar from sugarcane bagasse for wastewater treatment applications. Journal of Environmental Management 337: 117350.

29. Li X, Zhao Y, Zhou Q (2023) Nanobiochar for efficient heavy metal remediation: A review of mechanisms and performance. Science of the Total Environment 891: 164725.

30. Sharm A, Patel N, Verma S (2025) Role of surface charge and functionalization of nanobiochar in the adsorption of toxic metals from water. Environmental Research 249: 118899.

31. Wang Z, Liu D, Chen G (2024) Adsorption kinetics and isotherms of Pb (II) and Cu (II) using sugarcane bagasse-derived nanobiochar. Journal of Cleaner Production 435: 140567.

32. Thakur DS, Santosh NC (2025) Synthesis and characterization of coconut shell-based nanobiochar produced by controlled pyrolysis for dye adsorption from wastewater. Research & Development in Material Science 22(2): 2707-2718.

33. Zhang M, Huang Y, Xu L (2023) High-efficiency removal of Pb^{2+} and Zn^{2+} using sugarcane-derived nanobiochar: Mechanisms and environmental implications. Chemosphere 336: 139702.

34. Aziz KH, Kareem R (2023) Recent advances in water remediation from toxic heavy metals using biochar as a green and efficient adsorbent: A review. Case Studies in Chemical and Environmental Engineering 8: 100495.

35. Wang Y, et al. (2024) Research status, trends and mechanisms of biochar in pollutant remediation. Journal of Environmental Management, p. 122642.

36. Mei Y, Zhuang S, Wang J (2025) Adsorption of heavy metals by biochar in aqueous solution: A review. Science of the Total Environment 968: 178898.

37. Ullah MH, Rahman MJ (2024) Adsorptive removal of toxic heavy metals from wastewater using water hyacinth and its biochar: A review. Heliyon 10(17): e36869.

38. Mabaso T (2024) Effect of pyrolysis temperature on Pb (II) adsorption from water by biochar. Chemosphere, p. 141657.

39. Viotti P, Simone M, Angela A, María AD, Pietro L, et al. (2024) Biochar as alternative material for heavy metal adsorption from groundwaters: Lab-scale (column) experiment review. Materials 17(4): 809.